Source modelling insights from ground motion simulation validation of moderate magnitude active shallow crustal earthquakes in New Zealand

R.L. Lee, B.A. Bradley, J.M. Paterson & J.A. Motha

University of Canterbury, Christchurch

R.W. Graves

United States Geological Survey, Pasadena, CA, USA.

ABSTRACT

Hybrid broadband ground motion simulation validation has been an ongoing effort in NZ with recent studies focussed on active shallow crustal earthquakes of large magnitude ($M_w>7.0$) and small magnitude ($3.5<M_w\leq5.0$). Lessons from these studies have led to provisional modifications to the Graves and Pitarka (2010, 2015) simulation method and velocity modelling, both crustal and shallow, in the NZ context. Naturally the next step is to consider moderate M_w earthquakes ($5.0<M_w\leq7.0$) which bridge the gap between previous studies. Moderate M_w earthquakes, relative to small M_w earthquakes, introduce additional complexities in the simulations, due to their finite rupture size, that are important in the prediction of ground motions, which may have been previously obscured by the simplistic source modelling of small M_w earthquakes. This validation study considers 75 moderate M_w active shallow crustal earthquakes across NZ with 2042 ground motion records at 220 stations. The earthquake fault ruptures are kinematically modelled as single-plane finite faults given there are no detailed source inversion studies for these events (with few exceptions). The effect of fault dimension assumptions, kinematic slip generator, and choice of centroid moment tensor nodal plane on the simulated ground motions are examined. Comparisons with observed records through engineering intensity measures quantify the predictive capability of the simulations and examination of residuals highlight biases which are present in the prediction.

1 INTRODUCTION

Ground motion simulation validation efforts in New Zealand have previously been focused on large magnitude (M_w) earthquakes, such as the 2010 Darfield, 2011 Christchurch, and 2016 Kaikōura earthquakes (Bradley et

Paper 29

al., 2017, Razafindrakoto et al., 2018), due to their significance for earthquake engineering applications, as well as small M_w earthquakes (Lee et al., 2020, 2021) due to their relative simplicity and ubiquity which provided an opportunity to rigorously investigate systematic effects. This study presents source considerations for moderate M_w earthquake ground motion simulation validation, which aims to bridge the gap between previous validation studies. The simulation of moderate M_w earthquakes presents additional source nuances which are not apparent with small magnitude earthquakes and are therefore the focus of this study.

2   DATASETS AND SIMULATION METHOD

This study considers 75 moderate M_w earthquakes ($5.0 < M_w \leq 7.0$) with 2042 high-quality ground motion recordings across 220 stations, shown in Figure 1. Earthquake source descriptions were obtained from the GeoNet centroid moment tensor catalogue (Ristau, 2008). The quality of ground motions was determined using the ground motion quality classification neural network of Bellagamba et al. (2019).
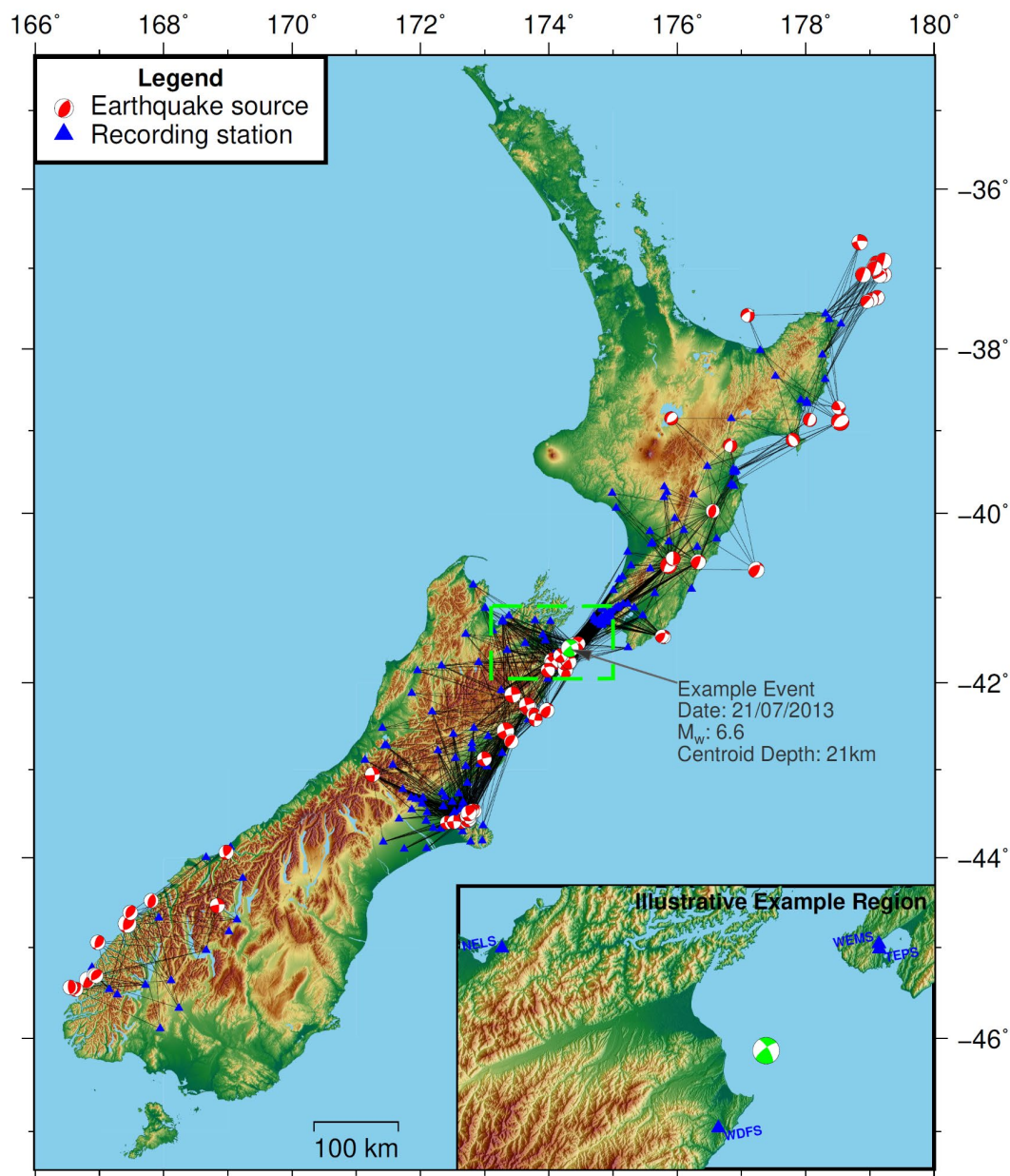

Figure 1: Map of New Zealand highlighting the 75 earthquake events, 220 recording stations and 2042 observed ground motion ray paths. The inset shows the specific region for the subsequent illustrative example.

Paper 29 – Source modelling insights from ground motion simulation validation of moderate magnitude…

Figure 2 illustrates the M_w and source-to-site distance (R_{rup}) distributions of the earthquakes and corresponding recorded ground motions. While there is a paucity of ground motions at $R_{rup} < 10$ km and $M_w > 6.2$, the remainder of the M_w-R_{rup} space of interest has relatively good coverage. As expected, there are generally more earthquakes at relatively smaller M_w (i.e., $M_w < 5.8$).
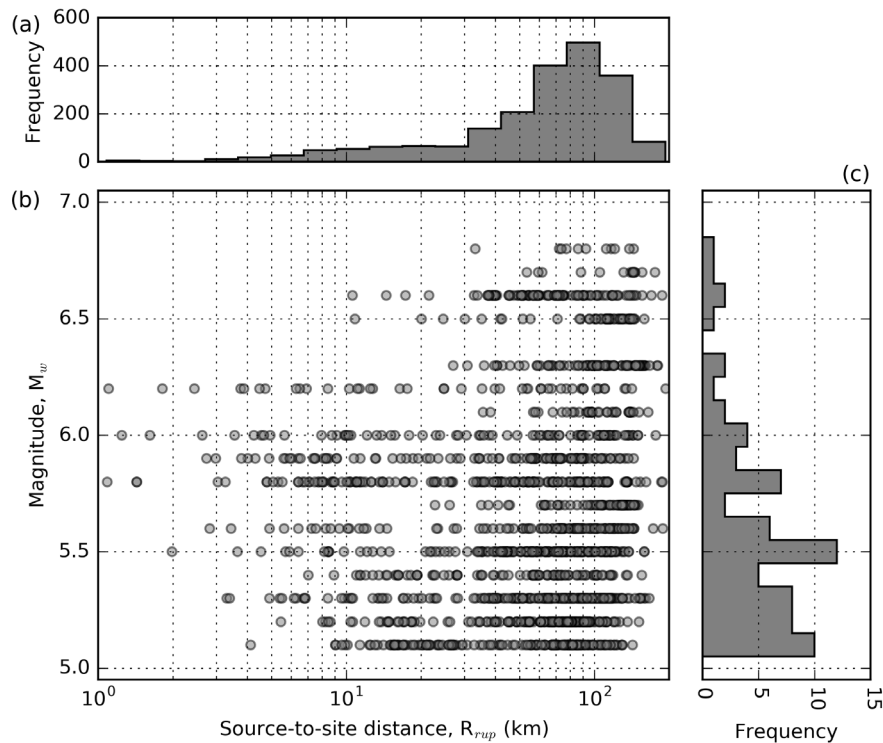

Figure 2: Earthquake source and ground motion dataset distributions: (a) record source-to-site distance histogram; (b) magnitude versus source-to-distance scatter plot; and (c) earthquake magnitude histogram.

This study utilises a 'Modified' Graves and Pitarka (2016) hybrid broadband ground motion simulation methodology. The broadband time series are a product of two parts, a comprehensive-physics low-frequency (LF) component and a simplified-physics high-frequency (HF) component. The LF component of the simulations use the NZVM (Lee et al., 2017, Thomson et al., 2020) to prescribe crustal velocity parameters for viscoelastic wave propagation. The HF component of the simulations use a generic 1D velocity model. The LF simulations are run with a finite difference grid spacing of 200 m and a minimum shear wave velocity of 500 m/s, yielding a maximum frequency of $f_t = 0.5$ Hz. Measured V_{s30} values are used where available for HF empirical site amplification, otherwise values are taken from an interim update of the Foster et al. (2019) national V_{s30} model.

3   KINEMATIC SOURCE MODELLING

For moderate M_w earthquakes, choices of source modelling assumptions can have significant impact on predicted ground motions as the rupture size becomes large. For comparison purposes, this study considers both point source and single-plane finite fault source models. Although point sources are likely not appropriate for moderate M_w earthquakes at this regional scale, it is still informative and provides a benchmark for comparisons. Two finite fault methods are considered which utilise the Leonard (2010) M_w-area scaling relationships (for rupture area and length-to-width aspect ratios) and various versions of the Graves and Pitarka (2010, 2016) kinematic rupture generator which produces spatially-variable slip, rise time and rake angle. These combinations are summarised in Table 1.

As the finite fault models used in this study have their geometry generated based on centroid moment tensor solutions (as detailed source inversion studies are not available for the majority of these earthquakes), the adopted solution of the two possible nodal planes can influence the simulated ground motions if finite rupture effects, such as directivity and seismic wave coherency, become significant. Figures 3a and 3b present example finite fault geometries of the two nodal planes for the 21st July 2013 M_w 6.6 Seddon Earthquake (highlighted in Figure 1) and Figure 3c shows the earthquake location for context. Through a comparison with the surrounding tectonic environment, it was deduced that the more appropriate nodal plane is the one shown in Figure 3b as the strike, dip and rake ($\phi = 233°$, $\delta = 75°$ and $\lambda = 162°$) are more consistent with the expected tectonic environment. This procedure was carried out for all 75 moderate M_w earthquakes considered in this study to identify the more appropriate nodal plane solution to be used in the simulations.

Figure 4 provides examples of two finite fault models for the 21st July 2013 M_w 6.6 Seddon Earthquake used in simulations shown subsequently, one for each of the adopted finite fault modelling methods. Kinematic distributions differ between the two methods as the rupture generators have different randomisation and spatial correlation algorithms. Method Finite Fault 2 also contains fault roughness (Shi and Day, 2013) which is not explicitly shown in Figure 4.

Table 1: Point source and finite fault source model parameters.

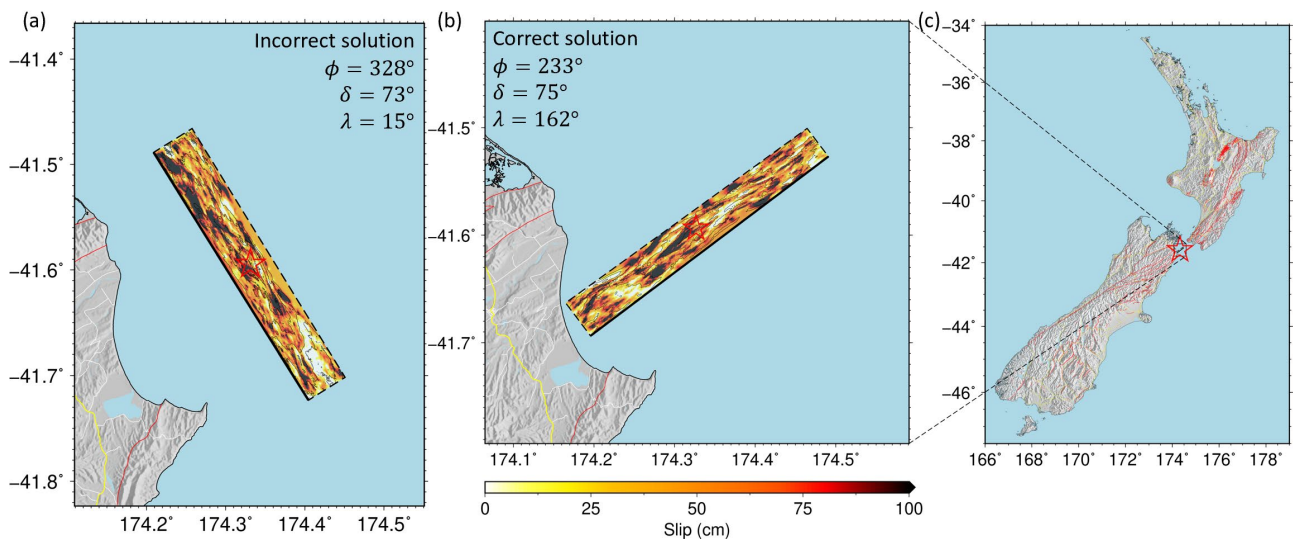| Method	M_w-Area Scaling	Slip Generator	Aspect Ratio	Fault Roughness	Figure
Point Source	Leonard (2010) for slip determination	N/A	N/A	N/A	N/A
Finite Fault 1	Leonard (2010)	genslip v3.3 (Graves and Pitarka, 2010)	Proportional to L/W (Leonard, 2010)	N/A	Figure 4a
Finite Fault 2	Leonard (2010)	genslip v5.4.2 (Graves and Pitarka, 2016)	Proportional to L/W (Leonard, 2010)	$\alpha = 0.01$	Figure 4b

Figure 3. Example finite fault geometries corresponding to the two possible centroid moment tensor nodal planes for the 21st July 2013 M_w 6.6 Seddon Earthquake: (a) incorrect solution; (b) correct solution; and (c) earthquake location within the NZ context. Red lines indicate known fault traces.

Paper 29 – Source modelling insights from ground motion simulation validation of moderate magnitude…
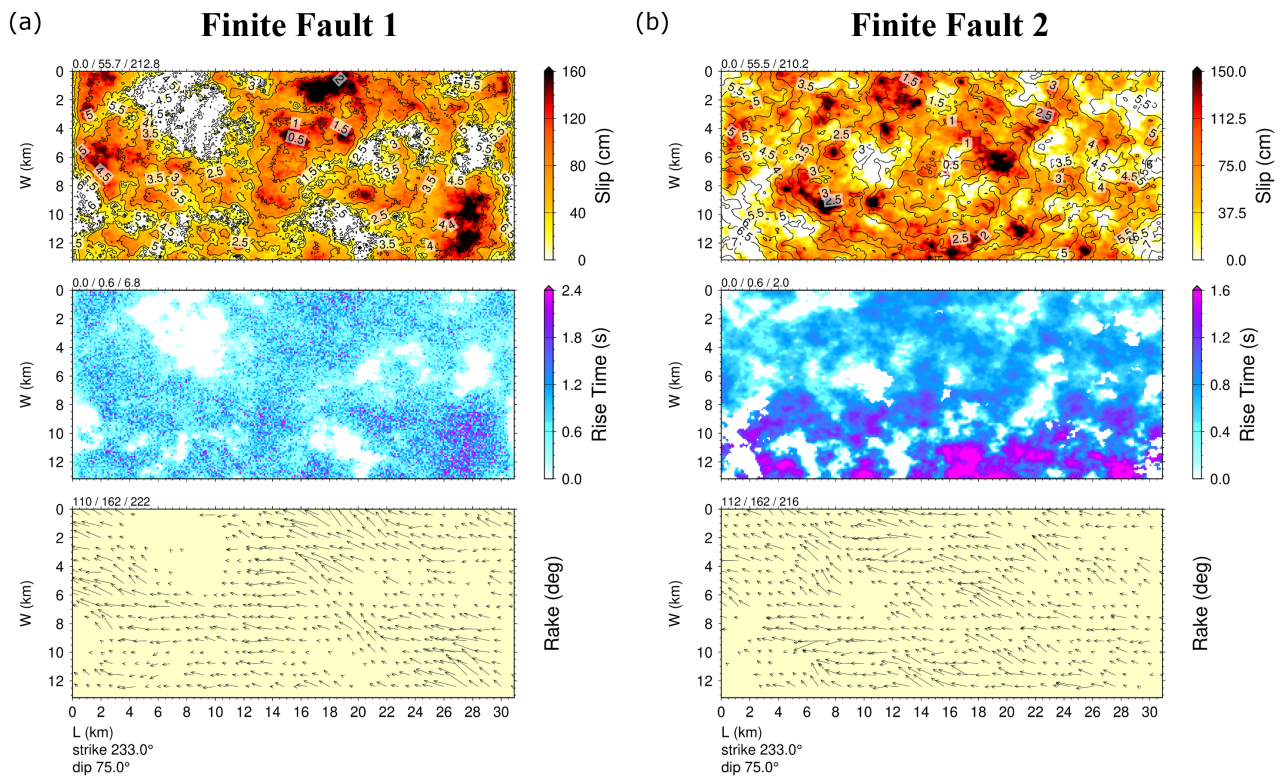
Figure 4: Examples of finite fault geometry and kinematic rupture parameter distributions - slip, rise time, and rake angle – for the 21st July 2013 Mw 6.6 Seddon Earthquake using method: (a) Finite Fault 1; and (b) Finite Fault 2.

4   ILLUSTRATIVE EXAMPLE SIMULATION

Ground motion simulations of the 21st July 2013 M_w 6.6 Seddon Earthquake are presented here to illustrate the salient attributes of the simulations. The finite fault simulations utilise the rupture models presented in the Kinematic Source Modelling section (Figure 4). Velocity waveforms are presented in Figure 5 for sites in Wellington, Nelson and Marlborough.

Overall, the point source simulation has stronger long period motion as a consequence of concentrated energy release in space and time causing excessive coherency. On the other hand, the finite fault simulations have energy release distributed over time and space resulting in lower peak amplitudes. The spatial randomisation of the kinematic source distributions would also contribute to uncertainty in the resulting finite fault simulation ground motions.

Figure 6 presents plots of PGA, pSA(3.0s) and D_{s595} as functions of source-to-site distance. The finite fault simulations tend to slightly underpredict PGA and D_{s595} while the point source simulation tends to significantly overpredict pSA(3.0s). Solid grey lines indicate commonly-used median empirical predictions and grey dashed lines are their ± 1 standard deviations.
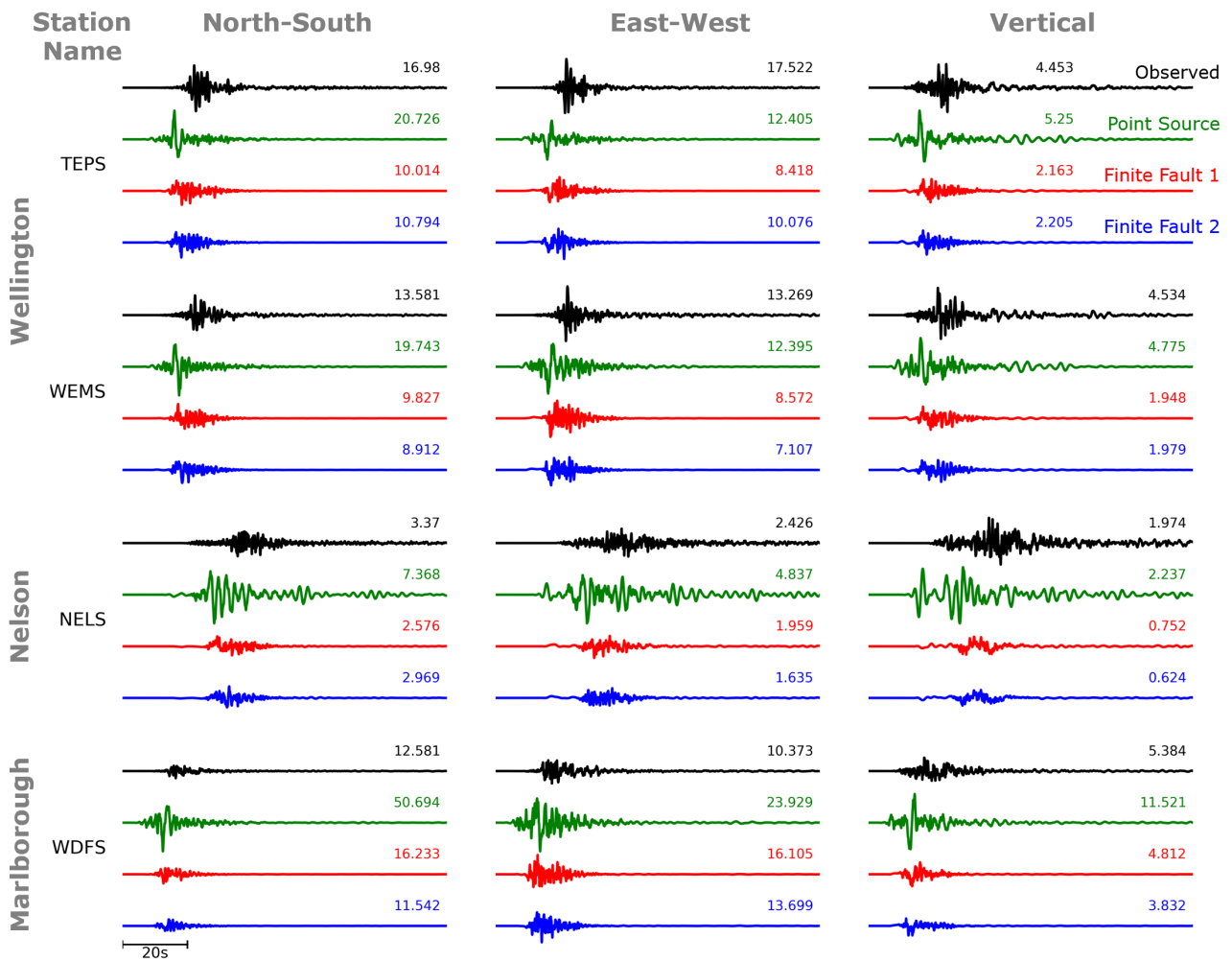
Figure 5: Observed (black), point source simulation (green), Finite Fault 1 simulation (red) and Finite Fault 2 simulation broadband velocity waveforms. PGV are provided to the right of each waveform in cm/s.
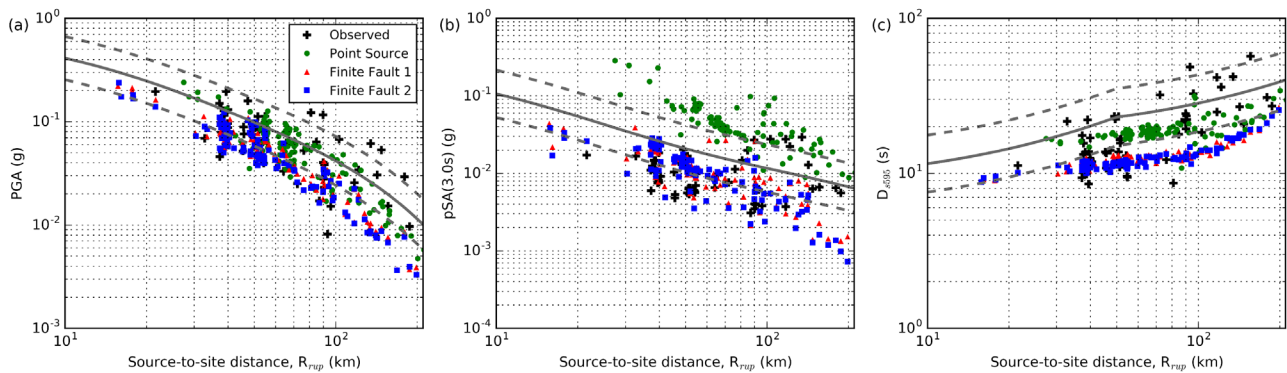

Figure 6: Observed and simulated intensity measures as a function of source-to-site distance: (a) PGA; (b) pSA(3.0s); and (c) D_{S595}. Solid grey lines are median empirical ground motion model predictions while dashed grey lines are $\pm 1\sigma$.

5   COMPLETE DATASET ANALYSIS

Figure 7 presents the model prediction bias and total standard deviation considering all records across the sources and sites considered. The point source simulations are found to systematically overpredict moderate-to-long period pSA while the finite fault simulations slightly underpredict at longer periods. The finite fault simulations have lower total standard deviation due to more appropriate modelling of the kinematic rupture.

While not shown, it is noted that an additional analysis was carried out using the incorrect centroid moment tensor nodal plane solutions (using the Finite Fault 2 method) to quantify the effect of incorrectly modelling this aspect. It was found that there was negligible effect on the model prediction bias but total standard deviations were larger by roughly 0.03 natural logarithm units. The majority of this difference is attributed to between-event variability. This is expected as the misfit for each ground motion would be larger due to incorrect source and path effects, but the overall bias would remain similar as resulting changes in overprediction would be offset by similar changes in underprediction given a reasonably well distributed dataset. The difference in standard deviation is modest as many of the faults still may not be considered large at this regional scale and hypocentres were assumed to be located at the fault centroid and therefore directivity effects are may be relatively small or not appropriately accounted for. Azimuthal or near source biases may exist and will be investigated in future work.
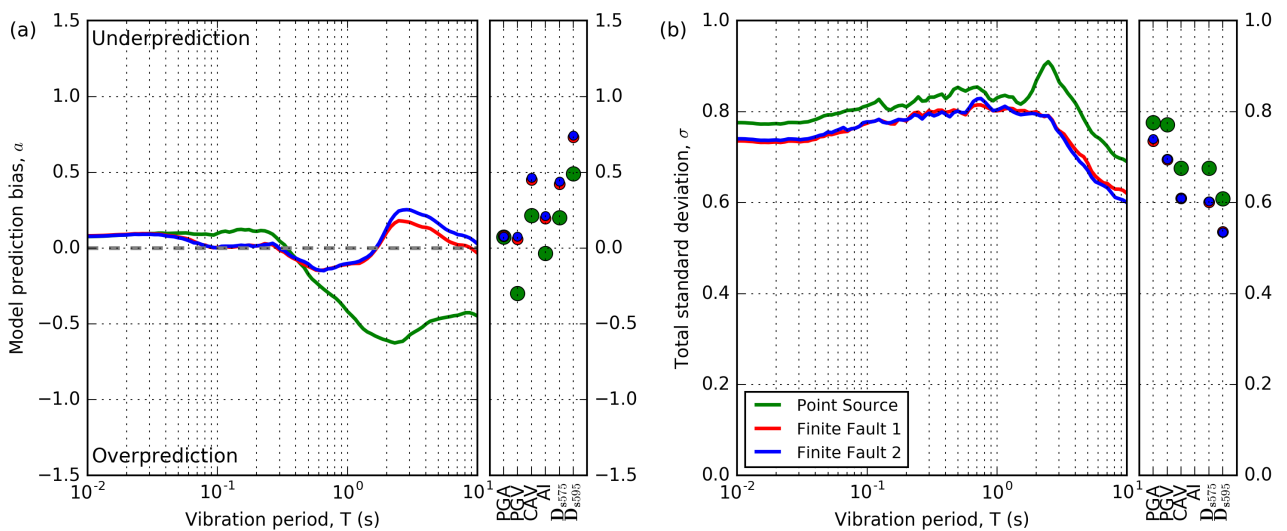

Figure 7: Ground motion simulation prediction summary: (a) systematic model prediction bias; and (b) total standard deviation.

6   CONCLUSIONS AND FUTURE WORK

This paper has presented preliminary results on ground motion simulation validation of active shallow crustal moderate M_w earthquakes in NZ. A key point illustrated was the limitations of modelling the kinematic rupture as a point source at the regional distances considered (with overprediction of long period pSA due to excessive coherency in seismic waves) which, while commonly understood, is rarely shown quantitatively. Finite fault models were preferred but presented additional challenges related to geometric and kinematic parameters. In particular, the choice of fault orientation, governed by choice of centroid moment tensor nodal plane in this study, resulted in small differences in ground motion variability as defined by the total standard deviation of the residuals. Different kinematic slip generators were found to cause larger differences in model prediction bias for long period pSA relative to short period pSA as spatial distribution and temporal evolution of slip has more influence on the comprehensive-physics LF simulation which models the kinematic rupture physics with greater detail.

Paper 29 – Source modelling insights from ground motion simulation validation of moderate magnitude…

The conclusions presented are mostly specific to the modelling choices and are therefore expected to change as the study progresses. Future work will consider additional aspects of source modelling such as other M_w-area scaling relationships, as well as utilise a recently updated version of the simplified-physics HF simulation method. LF simulations will also be run with higher resolution finite difference grid spacing (i.e., 100 m and 50 m to produce LF simulations with maximum frequencies of 1.0 Hz and 2.0 Hz, respectively) which would increase the period range corresponding to comprehensive-physics and better highlight the effect of fault roughness. As the kinematic rupture generators provide randomised distributions, several realisations of each earthquake will be necessary to obtain an averaged representation of the simulated ground motions.

7   REFERENCES

Bellagamba, X., Lee, R., & Bradley, B. A. (2019). A neural network for automated quality screening of ground motion records from small magnitude earthquakes. *Earthquake Spectra*, 35(4), 1637-1661.

Bradley, B. A., Razafindrakoto, H. N., & Polak, V. (2017). Ground-motion observations from the 14 November 2016 M w 7.8 Kaikoura, New Zealand, earthquake and insights from broadband simulations. *Seismological Research Letters*, 88(3), 740-756.

Foster, K. M., Bradley, B. A., McGann, C. R., & Wotherspoon, L. M. (2019). A V_{s30} Map for New Zealand Based on Geologic and Terrain Proxy Variables and Field Measurements. *Earthquake Spectra*, 35(4), 1865-1897.

Graves, R. W. and A. Pitarka (2010). Broadband ground-motion simulation using a hybrid approach, *Bulletin of the Seismological Society of America* 100(5A), 2095–2123.

Graves, R. and A. Pitarka (2015). Refinements to the Graves and Pitarka (2010) broadband ground-motion simulation method, *Seismological Research Letters* 86(1), 75–80.

Graves, R. and A. Pitarka (2016). Kinematic ground-motion simulations on rough faults including effects of 3D stochastic velocity perturbations, *Bulletin of the Seismological Society of America* 106(5), 2136–2153.

Lee, R. L., Bradley, B. A., Ghisetti, F. C., & Thomson, E. M. (2017). Development of a 3D Velocity Model of the Canterbury, New Zealand, Region for Broadband Ground-Motion Simulation. *Bulletin of the Seismological Society of America*, 107(5), 2131-2150.

Lee, R. L., Bradley, B. A., Stafford, P. J., Graves, R. W., & Rodriguez-Marek, A. (2020). Hybrid broadband ground motion simulation validation of small magnitude earthquakes in Canterbury, New Zealand. *Earthquake Spectra*, 36(2), 673-699.

Lee, R. L., Bradley, B. A., Stafford, P. J., Graves, R. W., & Rodriguez-Marek, A. (2021). Hybrid broadband ground motion simulation validation of small magnitude active shallow crustal earthquakes in New Zealand. *Earthquake Spectra*, (under internal review)

Leonard, M. (2010). Earthquake fault scaling: Self-consistent relating of rupture length, width, average displacement, and moment release. *Bulletin of the Seismological Society of America*, 100(5A), 1971-1988.

Razafindrakoto H.N.T., Bradley B.A., Graves R.W. (2018) Broadband ground-motion simulation of the 2011 M_w6.2 Christchurch earthquake, *New Zealand. Bulletin of the Seismological Society of America*. Vol. 108, No 4. pp. 2130-2147

Ristau, J. (2008). Implementation of routine regional moment tensor analysis in New Zealand, *Seismological Research Letters* 79(3), 400–415.

Shi, Z., & Day, S. M. (2013). Rupture dynamics and ground motion from 3-D rough-fault simulations. *Journal of Geophysical Research: Solid Earth*, 118(3), 1122-1141.

Thomson, E. M., Bradley, B. A., & Lee, R. L. (2020). Methodology and computational implementation of a New Zealand Velocity Model (NZVM2. 0) for broadband ground motion simulation. *New Zealand Journal of Geology and Geophysics*, 63(1), 110-127.